

# Detecting barriers to transport: A review of different techniques

G. Boffetta<sup>1</sup>, G. Lacorata<sup>2,3</sup>, G. Redaelli<sup>3</sup> and A. Vulpiani<sup>4</sup>

November 11, 2018

<sup>1</sup>Dipartimento di Fisica Generale and INFN, Università di Torino  
Via Pietro Giuria 1, 10125 Torino, Italy  
and Istituto di Cosmogeofisica del CNR, Corso Fiume 4, 10133 Torino, Italy.

<sup>2</sup>Dipartimento di Fisica, Università “La Sapienza”,  
Piazzale Aldo Moro 5, 00185 Roma, Italy.

<sup>3</sup>Dipartimento di Fisica, Università dell’ Aquila  
Via Vetoio 1, 67010 Coppito, L’Aquila, Italy.

<sup>4</sup>Dipartimento di Fisica, Università “La Sapienza”  
and INFN, Unità di Roma 1,  
Piazzale Aldo Moro 5, 00185 Roma, Italy.

## Abstract

We review and discuss some different techniques for describing local dispersion properties in fluids. A recent Lagrangian diagnostics, based on the Finite Scale Lyapunov Exponent (FSLE), is presented and compared to the Finite Time Lyapunov Exponent (FTLE), and to the Okubo-Weiss (OW) and Hua-Klein (HK) criteria. We show that the OW and HK are a limiting case of the FTLE, and that the FSLE is the most efficient method for detecting the presence of cross-stream barriers. We illustrate our findings by considering two examples of geophysical interest: a kinematic meandering jet model, and Lagrangian tracers advected by stratospheric circulation.

# 1 Introduction

Transport processes play a crucial role in many natural phenomena. Among the many examples, we just mention particle transport in geophysical flows which is of great interest for atmospheric and oceanic issues. The most natural framework for investigating such processes is the Lagrangian viewpoint, in which the tracer trajectory  $\mathbf{x}(t)$  is advected by a given Eulerian velocity field  $\mathbf{u}(\mathbf{x}, t)$  according to the differential equation

$$\frac{d\mathbf{x}}{dt} = \mathbf{u}(\mathbf{x}, t) \quad (1)$$

Despite of the simple formal relation (1), the problem of connecting the Eulerian properties of  $\mathbf{u}(\mathbf{x}, t)$  to the Lagrangian properties of the trajectories  $\mathbf{x}(t)$ , and *viceversa*, is a very difficult task. In the last 20 – 30 years the scenario has become even more complex by the recognition of the ubiquity of Lagrangian chaos (chaotic advection). Even very simple Eulerian fields can generate unpredictable Lagrangian trajectories which are practically indistinguishable from those obtained in a complex, turbulent, flow [1, 2, 3, 4].

In the following we will restrict our attention to the case of two-dimensional incompressible velocity field  $\mathbf{u}(\mathbf{x}, t)$ , with  $\mathbf{x} = (x, y)$ . Incompressibility is automatically satisfied by introducing the stream function  $\psi = \psi(\mathbf{x}, t)$  and consequently defining the velocity field in terms of partial derivatives as  $\mathbf{u} = (\psi_y, -\psi_x)$ . The evolution equation (1) then becomes

$$\frac{dx}{dt} = \psi_y, \quad \frac{dy}{dt} = -\psi_x. \quad (2)$$

Formally (2) is a Hamiltonian system with Hamiltonian  $\psi(\mathbf{x}, t)$ . Chaotic trajectories  $\mathbf{x}(t)$  typically appear as a consequence of the time dependence of  $\psi$  [2].

Many geophysical flows, when observed at sufficiently large scale, are within this class [5, 6]. Moreover time dependence can be often considered a perturbation over a given steady flow, i.e. (2) represents a quasi-integrable Hamiltonian system. It is well known that in quasi-integrable Hamiltonian systems chaos can be quite non uniform in the phase space, due to the presence of the invariant KAM tori with a chaotic layer around them [3]. The presence of these regular islands (also called coherent structures in the context of geophysical flows) is of particular importance for the dispersion process because they act as barriers to transport. The sensitivity of different

diagnostics of transport to the presence of barriers will be the main topic of our investigation. In particular, we will consider the Finite Time Lyapunov Exponent (FTLE), the Okubo-Weiss (OW) and Hua-Klein criteria (HK), and the local Finite Scale Lyapunov Exponent (FSLE).

We discuss these different methods by considering two examples. First, we study transport properties in a kinematic meandering jet model, formerly introduced for describing the Gulf stream [7, 5]. Second, we analyze a large number of stratospheric isentropic trajectories, computed according to (1) from assimilated wind fields, describing Lagrangian motion around the polar vortex. In both situations our results show that the existence of barriers limiting the dispersion across the stream is well described by the FSLE but it is completely missed by the OK and HK criteria, which can only depict the landscape of alternating unstable hyperbolic and stable elliptic points of the flow. The FTLE will be discussed in relation to the OW and HK exponents and to the FSLE.

The remaining of this paper is organized as follows. In Section 2 we introduce and discuss the different diagnostics for characterizing dispersion. Section 3 is devoted to the analysis of the meandering jet and of the polar vortex. Finally, in Section 4 we present some conclusions.

## 2 Characterization of local transport properties

In presence of Lagrangian chaos, two close trajectories typically separate exponentially in time [4]. Thus the natural statistics we adopt for describing chaotic particle spreading is the relative dispersion statistics. Relative separation between two particles  $\mathbf{R}(t) = \mathbf{x}'(t) - \mathbf{x}(t)$  evolves according to the velocity difference

$$\frac{d\mathbf{R}}{dt} = \mathbf{u}(\mathbf{x}(t) + \mathbf{R}(t), t) - \mathbf{u}(\mathbf{x}(t), t). \quad (3)$$

As far as particle separation remains much smaller than the typical length scale  $l_E$  of the velocity field, we can linearize (3) around the trajectory  $\mathbf{x}$  and, for a generic time dependent flow, we expect exponential growth of the separation, i.e.

$$R(t) \simeq R(0)e^{\lambda t} \quad (4)$$

where  $\lambda$  is the Lagrangian Lyapunov Exponent (LE).

In the opposite limit,  $R \gg l_E$ , the two particles feel uncorrelated velocity fields and one recovers the standard diffusive regime, i.e.

$$\langle R^2(t) \rangle \simeq 2Dt \quad (5)$$

where the average is taken over many particle pairs and where  $D$  is the diffusion coefficient.

It is important to remark that, in most realistic situations, both asymptotic regimes, i.e. very small  $R(t)$  for (4) and very large  $R(t)$  for (5) cannot be attained. From one side, particles separation can be not sufficiently small to justify the linearization leading to (4). In the opposite limit, large separations cannot be reached in presence of boundaries at scales comparable with  $l_E$ . As a consequence, the asymptotic quantities as  $\lambda$  and  $D$  cannot be computed and a non-asymptotic characterization of transport is needed [8].

Let us discuss, now, some techniques one can use to characterize local dynamical properties of a system, in particular the relative dispersion rate as a function of the initial position.

## 2.1 The Finite Time Lyapunov Exponent

Let us start from the definition of the Lagrangian Lyapunov Exponent:

$$\lambda = \lim_{t \rightarrow \infty} \lim_{R(0) \rightarrow 0} \frac{1}{t} \ln \frac{R(t)}{R(0)} \quad (6)$$

In (6) one basically assumes that the linearization of the perturbation  $R(t)$  on a generic reference trajectory holds for an infinite time. This is correct only if the perturbation can be considered infinitesimal at any time. The characteristic time naturally associated to the LE is known as the predictability time  $T_\lambda = \lambda^{-1}$ , which is the characteristic time at which one can predict the position of the tracer in the future. The FTLE is obtained by avoiding the limit  $t \rightarrow \infty$  in (6). This gives the instantaneous growth rate over a finite interval  $\tau$  as

$$\gamma_\tau(t) = \lim_{R(t) \rightarrow 0} \frac{1}{\tau} \ln \frac{R(t+\tau)}{R(t)} \quad (7)$$

which, at variance with  $\lambda$ , depends on the initial point  $\mathbf{x}(t)$ . The FTLE is distributed around a mean value which is nothing but the LE,  $\langle \gamma_\tau \rangle = \lambda$ ,

where the average is computed over a virtually infinite number of  $\tau$  intervals along the trajectory [11].

In principle, even at very small  $R(t)$ , one must wait a certain time interval,  $T_w$ , needed to drive the perturbation along the Lyapunov direction [12]. This is necessary if we want to measure intrinsic properties of the system. In presence of many degrees of freedom, the possibility that the waiting time  $T_w$  is of the same order of the predictability time  $T_\lambda$  cannot be excluded (see [9] for a review on the predictability time in extended systems).

Let us now discuss some practical shortcomings arising when we want to analyze realistic situations described by experimental or model data. First, as we already rescaled, in quasi-integrable Hamiltonian systems, different regions in the phase space can display different behaviors [2]. As a consequence one has a non trivial spatial distribution of Lyapunov exponents: zero if the trajectory lies in a regular island, positive if it diffuses across the stochastic layer. In special cases, when for instance structures of the velocity field are “localized” persistent features, at least within time intervals considerably longer than the characteristic Lagrangian time, a more refined description in terms of finite-time Lyapunov exponent can be more appropriate.

In order to measure  $\gamma_\tau(t)$  at a point  $\mathbf{x}(t)$  one can make use of the following procedure. Backward integration in time for an interval  $T_*$  bring the trajectory at the point  $\mathbf{x}(t - T_*)$ . An infinitesimal perturbation  $\delta\mathbf{x}(t - T_*)$  is switched on and it is integrated forward to  $\delta\mathbf{x}(t)$ . If  $T_*$  is sufficiently long, i.e.  $T_* \geq T_w$ , the perturbation  $\delta\mathbf{x}(t)$  will be aligned along the Lyapunov eigenvector and a further integration to  $\delta\mathbf{x}(t + \tau)$  will give the FTLE according to (7) [12]. In general,  $T_w$  is not known *a priori* and can vary with the initial conditions. More serious problems arise from the limits of resolution in the knowledge of experimental or simulated Lagrangian data, which can easily disrupt the linear approximation scenario.

When  $R(t)$  attains finite sizes, i.e. is of the order of the characteristic lengths of the system, the so-called Finite-Scale Lyapunov Exponent (FSLE) give an appropriate description of the intrinsic physical properties of dispersion at different scales of motion. We will discuss this point in Section 2.3.

## 2.2 The Okubo-Weiss and Hua-Klein criteria

In two-dimensional turbulent flows, the stirring properties of initially small material lines are related to the combined effect of eddy and jet features of

the velocity field. In cases when continuous velocity fields are given, a popular way used to characterize the local rate of separation of initially close trajectories is the Okubo-Weiss (OW) criterion [13, 14], based on the computation of the eigenvalues of the velocity gradient tensor. If explicit time dependence cannot be neglected, Hua and Klein (HK) [10] have proposed a generalization of the OW criterion, based on the computation of the eigenvalue of the acceleration gradient tensor, related to the distribution of the pressure field.

Let us recall the two criteria in the case of 2D incompressible velocity field with Lagrangian evolution given by (2). The evolution of an infinitesimal separation  $\mathbf{R}(t)$  is given in the tangent space as

$$\frac{d\mathbf{R}}{dt} = \begin{pmatrix} \psi_{xy} & \psi_{yy} \\ -\psi_{xx} & -\psi_{xy} \end{pmatrix} \mathbf{R} \equiv \mathbf{M}\mathbf{R}, \quad (8)$$

where the Jacobian  $\mathbf{M}$  has the property  $\mathbf{M}^2 = \lambda_0 \mathbf{1}$  with  $\lambda_0 = -\det(\mathbf{M})$ . At small times, the solution of (8) is

$$\mathbf{R}(t) = \left[ \mathbf{1} + \mathbf{M}t + \frac{1}{2}\mathbf{N}t^2 \right] \mathbf{R}(0) + O(t^3) \quad (9)$$

where  $\mathbf{N} = \lambda_0 \mathbf{1} + d\mathbf{M}/dt$ . The Okubo-Weiss criterion consists in computing  $\lambda_0$ , i.e. the product of the eigenvalues of  $\mathbf{M}$ . We recall that the quantity  $\lambda_0$  can be written in terms of the square strain  $\sigma^2$  and the square vorticity  $\omega^2$  as

$$\lambda_0 = \frac{1}{4}(\sigma^2 - \omega^2) \quad (10)$$

If  $\lambda_0$  is positive, the two eigenvalues of  $\mathbf{M}$  are real, the velocity field is locally hyperbolic and strain overcomes rotation. For negative  $\lambda_0$ , we have imaginary eigenvalues and a predominance of rotation over strain.

Of course, the Okubo-Weiss criterion may not be sufficient to determine the local strain-vorticity balance in a time dependent flow. In this respect, the Hua-Klein criterion, being based on the sign of the largest eigenvalue of the  $\mathbf{N}$  matrix  $\lambda_+ = \lambda_0 + \lambda_1$ , with

$$\lambda_1 = \sqrt{\frac{d\psi_{xy}}{dt}^2 - \frac{d\psi_{xx}}{dt} \frac{d\psi_{yy}}{dt}} \quad (11)$$

gives a ‘‘more Lagrangian’’ description. Both of them provide a picture of the distribution of stable elliptic points and unstable hyperbolic points in the

flow. Let us observe that in the case of stationary velocity field,  $d\mathbf{M}/dt = 0$  and one has  $\lambda_+ = \lambda_0$ .

Let us remark the relationship existing between the HK criterion and the FTLE. The “instantaneous” Lyapunov exponent  $\gamma_\tau$  estimates the growth rate of a typical perturbation within a finite time interval  $\tau$ , after the perturbation has aligned along the most unstable direction, so that it is an intrinsic property shared by all the trajectories (except for a set of zero probability measure). The HK eigenvalue  $\lambda_+$  estimates the local maximum strain rate, regardless any alignment time of the perturbation, so that, from the Lagrangian point of view, it may be biased by transient behaviors. In other words, measuring  $\lambda_+$  corresponds to measuring  $\gamma_\tau$  at very small  $\tau$  (the integration time step) starting with a perturbation always aligned along the locally most unstable direction. In practical situations it can happen that the HK eigenvalue and the FTLE give similar local descriptions but, from a theoretical point of view, starting with a perturbation along the local most unstable direction is as arbitrary as choosing any other direction: after a transient, the time evolution will drive the (infinitesimal) perturbation definitely along the most unstable Lyapunov eigenvector.

### 2.3 The local Finite Scale Lyapunov Exponent

In most cases of interest, the linear regime during which the exponential growth of the inter-particle distance occurs can be not resolved. Particle spreading is generally observed on large spatial scales, of the order of the characteristic lengths of the system, and appropriate non linear techniques must be employed to quantify relative dispersion rates (see [15] for a review about non asymptotic properties of transport and mixing).

Let us consider a very small (infinitesimal) initial perturbation  $R(0)$  on a trajectory  $\mathbf{x}$ . For a chaotic system, after the initial transient,  $R(t)$  typically grows exponentially in time according to (4). We wait until  $R(t)$  reaches a certain threshold  $\delta_i$ , at a given time  $t_i$ . Let  $\mathbf{x}_i$  the position of the trajectory  $\mathbf{x}$  at time  $t_i$ . At a later time  $t_f$ ,  $R(t)$  will reach a larger threshold  $\delta_f = r \cdot \delta_i$  with an assigned  $r > 1$ . We now define the  $r$ -amplification time of  $R(t)$ , relatively to the initial position  $\mathbf{x}_i$ , as  $\tau(\delta_i, \mathbf{x}_i, r) = t_f - t_i$ . From this quantity,

the local Finite Scale Lyapunov Exponent is defined as:

$$\lambda_r(\delta_i, \mathbf{x}_i) = \frac{1}{\tau(\delta_i, \mathbf{x}_i, r)} \ln r \quad (12)$$

The exponent  $\lambda_r(\delta_i, \mathbf{x}_i)$  is a measure of the local amplification rate of a perturbation of size  $\delta_i$  on a trajectory passing by the point  $\mathbf{x}_i$ . In the case of periodic time dependence in the equation of motion, the local FSLE will depend also on the initial phase.

The above described prescription is necessary in order to characterize the perturbation growth as an intrinsic property of the system. Of course, in realistic situations, we have to consider the following problems: the flow is not simply periodic and thus  $\lambda_r$  may depend explicitly on time. Moreover, we cannot observe distances below a certain threshold because of finite resolution, and thus the initial perturbation cannot be considered infinitesimal. Another important remark is that in practical applications it may not be possible to have information on a uniform distribution of initial conditions. In particular, let us consider a 2-D time dependent velocity field (e.g. the surface circulation of a sea or an isentropic layer of the stratosphere) and the relative Lagrangian dispersion of trajectories. Usually one cannot set the initial distance between two particles to an arbitrarily small size, and wait until the relative position vector is aligned with the most unstable direction and starts expanding with a typical rate measured by the LE. Finite resolution imposes a lower limit to physically reasonable distance sizes, say  $\delta$ , and we can only hope to take into account all the possible realizations of the local dispersion rate by taking the average of  $\lambda_r(\delta, \mathbf{x})$  ( $r > 1$ ) over a large number of directions around the initial point  $\mathbf{x}$ , i.e. on a sphere with radius  $\delta$ . Furthermore, if  $\delta$  is not very small if compared to the characteristic lengths of the system, the linear regime of instability is already expired. The FSLE, by its nature, is a non linear indicator of trajectory instability so it can measure relative dispersion rates at finite scales of motion. How long can we follow two trajectories so that their FSLE is still meaningful as a local diagnostics? The answer depends essentially on how much rapidly the velocity field varies in time relatively to the Lagrangian characteristic time. For instance, if  $T_E$  is the time scale within which the Eulerian structures, e.g. current systems, change their geometrical and physical aspects, local FSLE's are meaningful only if they are observed on times  $\ll T_E$ , i.e. in an almost *frozen field* approximation.



Let us now briefly discuss the main objective of the present paper, i.e. the detection of barriers in particle transport. We seed the flow with an uniform distribution of Lagrangian tracers and compute the FSLE for any trajectory according to the prescription given above.

If  $\ell_E$  represents some characteristic length in the flow, e.g. the typical size of the eddies around the Gulf Stream in the North Atlantic Ocean or around the polar jet current in the stratosphere, then particles trapped inside vortices or traveling down jet streams may never separate beyond the scale  $\ell_E$ , giving  $\lambda_r(\delta) = 0$  for  $\delta \leq \ell_E$ . On the contrary, particles located in the chaotic layer will give a positive FSLE. Thus at an appropriate value of the threshold  $\delta$ , the map of FSLE (12) can be used as an efficient indicator of the presence of barriers in transport.

We will see how a simple periodically perturbed meandering jet can be a significant test to show that a more appropriate diagnostics is required when macroscopic barriers are under investigation. An interesting result related to geophysical data analysis concerns the barrier effects of the jet current of the stratospheric polar vortex (southern hemisphere). This technique is being used also to study local mixing properties in ocean systems.

## 3 Results

### 3.1 Numerical experiments

We first discuss a simple, but not trivial, kinematic model in which a barrier to motion is known to exist for certain values of the parameters. The transition to the barrier-breakdown occurs by variation of some parameters. We use this model to show what kind of information can be extracted from the different techniques previously discussed. The system, formerly introduced as a model of transport across the Gulf Stream [7, 5], consists a time periodic streamline pattern forming an oscillating meandering (westerly) current with recirculations along its boundaries:

$$\Psi = -\tanh \left[ \frac{y - B \cos kx}{\sqrt{1 + k^2 B^2 \sin^2 kx}} \right] + cy \quad (13)$$

where  $k$  is the spatial wave number of the structure,  $c$  is the retrograde velocity in the “far field”,  $B$  is the amplitude of the meanders which varies

periodically in time as

$$B = B_0 + \epsilon \cos(\omega t + \phi) \tag{14}$$

The system can be fully mixing, i.e. any portion of the domain is definitely visited from any initial condition, in a certain portion of the parameter space  $(\epsilon, \omega)$  where in particular one has cross stream transport. This system has two separatrices, with a spatial periodic structure, see Fig. 1, coinciding with the borderlines of the current. At very small  $\epsilon$  the chaotic layer is restricted to a limited region around the separatrices, and no cross stream mixing occurs. In order to have large-scale chaotic mixing, i.e. particles jumping across the jet from a northern recirculation to a southern one, and vice-versa, one needs the overlap of the resonances [16], when  $\epsilon$  and  $\omega$  are larger than certain critical thresholds.

In Figure 3 we report the OW indicator  $\lambda_0(\mathbf{x})$  as function of the initial position. Incidentally, the HK indicator  $\lambda_+(\mathbf{x})$  shows no significant differences from  $\lambda_0$  and it is not shown. It is important to observe that both the OW and HK criteria are not able to detect the existence or not of a dynamical barrier, i.e. the two figures are practically indistinguishable.

The finite time Lyapunov exponent  $\gamma_\tau(\mathbf{x})$  is shown in Figure 4. The computation is done according to (7) with initial separation  $R(t) = \delta$  for all the particle pairs, without the “waiting procedure” (i.e.  $T_w = 0$ ). This is because we want to mimic a realistic situation of data analysis in which arbitrarily small separations cannot be attained.

We note that, although the indicator is able to detect the jet core (the low FTLE value filament inside the chaotic current), the transition between the confined chaos regime and the large scale mixing regime is not observed (compare Figure 4a and Figure 4b). The asymmetry of the FTLE map is due to the dependence of this indicator on the initial phase of the periodic flow.

Let us consider the local FSLE as  $\lambda_r(\mathbf{x})$ , computed on the same trajectories and with the same initial separation of Figure 4. Figure 5 contains the results of the  $\lambda_r$  maps, before and after the overlap of the resonances, in what we can call the Melnikov [17] and the Chirikov [16] regimes, respectively. The amplification factor  $r$  and the lower threshold  $\delta$  are chosen such that the upper threshold  $r \cdot \delta$  is of the order of the jet width. In one case, black regions of zero FSLE values, i.e. particle pairs which never reach the

upper limiting separation, are located in the jetcore and in the centers of the recirculation: when chaos is still confined in the vicinity of the separatrices, no cross-stream transport is allowed. In the other case, after the separatrix breaking has occurred, no zero FSLE values are present, indicating that particles can spread apart over any distance from any initial condition.

Let us conclude this section by remarking that a Lagrangian diagnostic based on the FSLE shows is major skill in detecting dynamical barriers in the flow.

## 3.2 Geophysical data

We now consider a geophysical example regarding Lagrangian motion on an isentropic layer (i.e. at constant potential temperature) at a low stratospheric level, in presence of the wintery polar vortex [19], characterized by a quasi-zonal robust jet stream.

The typical flow pattern is usually represented by means of stereographic maps of isentropic Potential Vorticity (PV), see Figure 6, and the modulus of its gradient shown in Figure 7. In winter, the stratospheric PV can be considered as a quasi-conserved quantity over a timescale of about 2-3 weeks. It is also widely accepted in literature that the outer border of the polar vortex, usually identified by the maximum horizontal gradient of isentropic PV [22], can act as a strong barrier to meridional cross stream transport.

The kinematics is remarkably similar to that of the previously discussed meandering jet model, if we imagine the latter as closed on itself in a circular geometry. The Lagrangian data set we have used for the analysis account of about  $10^4$  trajectory pairs, initially uniformly distributed over the southern hemisphere on the 475K isentropic surface (lower stratosphere). Trajectories are calculated by means of the University of L'Aquila Trajectory Model [21, 24] using analyzed wind, pressure, and temperature fields from the U.K. Meteorological Office (UKMO) [20] provided by the British Atmospheric Data Centre (BADC). Latitude coverage goes from poles to about tropics. The trajectories run from June 30th, 1997 up to a maximum observation time of 20 days. The initial distance between pair particles is  $R_i \simeq 10 \text{ Km}$ .

Being the trajectory evolution simulated with wind fields relative to the southern hemisphere wintery season, we are observing a situation of stable polar vortex regime [23].

The local properties of the particle relative dispersion are obtained by computing the Okubo-Weiss eigenvalue  $\lambda_0$  and the local FSLE  $\lambda(r)$ . Spatial derivatives of the velocity fields used for the calculations are estimated as finite differences over spatial grid steps of the order of  $100 \text{ Km}$ .

The results are presented in the two-dimensional maps in Figures 8 and 9. A further analysis (not shown) demonstrates that  $\lambda_0$  does not change substantially in time and, as a consequence, it reproduces the essential features of the HK exponent  $\lambda_+$ . Neither of the exponents, as in the previous example, is able to detect the presence of a barrier to transport.

On the other hand, the FSLE map (see Figure 9) detects the dynamical barrier as the region of vanishing FSLE values. The location of the barrier is in good agreement with the definition of polar vortex border based on geophysical considerations, e.g. the potential vorticity gradient shown in Figure 7 [22].

## 4 Conclusions

We have discussed several techniques proposed for describing dispersion in two-dimensional flows. In particular our analysis has been focused on the capability of these techniques to detect the presence of barriers to transport. By means of two examples of geophysical relevance, we have shown that Eulerian-based techniques, such as the Okubo-Weiss criterium and its generalization proposed by Hua and Klein, are not sensible to the presence of barriers. The Lagrangian finite-time Lyapunov exponent is, in principle, useful for describing space variations of the chaotic properties, e.g. in a quasi-integrable Hamiltonian system, but it is limited to small-scale properties of dispersion. A recent non-linear Lagrangian diagnostics, based on the Finite Scale Lyapunov Exponent, is found to give the correct description of the presence of large-scale barriers. As final remark, we notice that the OW criterion has been recently shown to give poor information also in the case of fully developed turbulence [18]: the probability distribution function of  $\lambda_0$ ,  $P(\lambda_0)$ , for a typical 2D turbulent field is not sensitive to the presence of coherent structures, i.e.  $P(\lambda_0)$  is the same as for a Gaussian field.

From a general point of view, it is not a surprise that purely Eulerian statistics, such as the OW quantity, are unable to predict the behavior of Lagrangian tracers. The presence of dynamical barriers is a fundamental

information about the transport properties of the flow and thus can be considered as a good discriminatory for the diagnostics. It would be interesting to check the performance of the proposed methods on other geophysical flows.

We thank the British Atmospheric Data Center for the UKMO data. We are grateful to B. Joseph, D. Iudicone, B. Legras, R. Santoleri and G. Visconti for useful discussions. This work is partially supported by MURST (contract N. 9908264583).

## References

- [1] M. Hénon, Sur la Topologie des Lignes de courant dans in cas particulier, C. R. Acad. Sci. Paris A 262 (1966) 312.
- [2] A.J. Lichtenberg and M.A. Lieberman, Regular and Stochastic Motion (Springer, Berlin 1982).
- [3] J.M. Ottino, The kinematics of mixing: stretching, chaos and transport (Cambridge University Press, Cambridge 1989).
- [4] A. Crisanti, M. Falcioni, G. Paladin and A. Vulpiani, Lagrangian Chaos: Transport, Mixing and Diffusion in Fluids, Riv. Nuovo Cim. 14 (1991) 1.
- [5] R.M. Samelson, Fluid exchange across a meandering jet, J. Phys. Oceanogr. 22 (1992) 431.
- [6] H. Yang, Chaotic transport and mixing by ocean gyre circulation, in Stochastic modeling in physical oceanography (ed. by R.J. Adler, P. Muller and B.L. Rozovskii) Birkhäuser (1996) 439.
- [7] A.S. Bower, A simple kinematic mechanism for mixing fluid parcels across a meandering jet, J. Phys. Oceanogr. 21 (1991) 173.
- [8] V. Artale, G. Boffetta, A. Celani, M. Cencini and A. Vulpiani, Dispersion of passive tracers in closed basins: beyond the diffusion coefficient, Phys. Fluids 9 (1997) 3162.
- [9] T. Bohr, M. H. Jensen, G. Paladin and A. Vulpiani, Dynamical systems approach to turbulence (Cambridge University Press, Cambridge 1998).
- [10] B.L. Hua and P. Klein, An exact criterion for the stirring properties of nearly two-dimensional turbulence, Physica D 113 (1998) 98.
- [11] G. Boffetta, M. Cencini, M. Falcioni and A. Vulpiani, Predictability: a way to characterize complexity, Phys. Report (submitted, 2001).
- [12] I. Goldrisc, P.L. Sulem and S.A. Orszag, Stability and Lyapunov stability of dynamical systems: a differential approach and a numerical method Physica D 27 (1987) 311.

- [13] A. Okubo, Horizontal dispersion of floatable particles in the vicinity of velocity singularities such as convergences, *Deep-Sea Res.* 17 (1970) 445.
- [14] J. Weiss, The dynamics of enstrophy transfer in two-dimensional hydrodynamics, *Physica D* 48 (1991) 273.
- [15] G. Boffetta, A. Celani, M. Cencini, G. Lacorata and A. Vulpiani, Nonasymptotic properties of transport and mixing, *Chaos* 10 (2000) 50.
- [16] B.V. Chirikov, A universal instability of many-dimensional oscillator systems, *Phys. Rep.* 52 (1979) 263.
- [17] V.K. Melnikov, On the stability of the center for time periodic perturbations, *Trans. Moscow Math. Soc.* 12 (1963) 1.
- [18] M. Rivera, X. L. Wu and C. Yeung, Universal Distribution of Centers and Saddles in Two-Dimensional Turbulence, (preprint, arXiv:physics/0012051, 2001).
- [19] M.R. Schoeberl, L.R. Lait, P.A. Newman and J.E. Rosenfield, The structure of the polar vortex, *J. Geophys. Res.* 97 (1992) 7859.
- [20] R. Swinbank and A. O'Neill, A stratosphere-troposphere data assimilation system, *Mon. Weather Rev.* 122 (1994) 686.
- [21] G. Redaelli, Ph. D. Dissertation, University of L'Aquila, 1997.
- [22] E.R. Nash, P.A. Newman, J.E. Rosenfield and M. R. Scheberl, An objective determination of the polar vortex using Ertel's potential vorticity, *J. Geophys. Res.* 101 (1996) 9471.
- [23] M. Schoeberl and Hartmann D. L., The dynamics of the Stratospheric Polar Vortex and its relation to springtime ozone depletions, *Science* 251 (1991) 45.
- [24] R. Dragani, G. Redaelli, G. Visconti, A. Mariotti, V. Rudakov, A. R. MacKenzie and L. Stefanutti, High resolution stratospheric tracer fields reconstructed with lagrangian techniques: a comparative analysis of predictive skill, *J. of Atmos. Sci.* (in press, 2001).

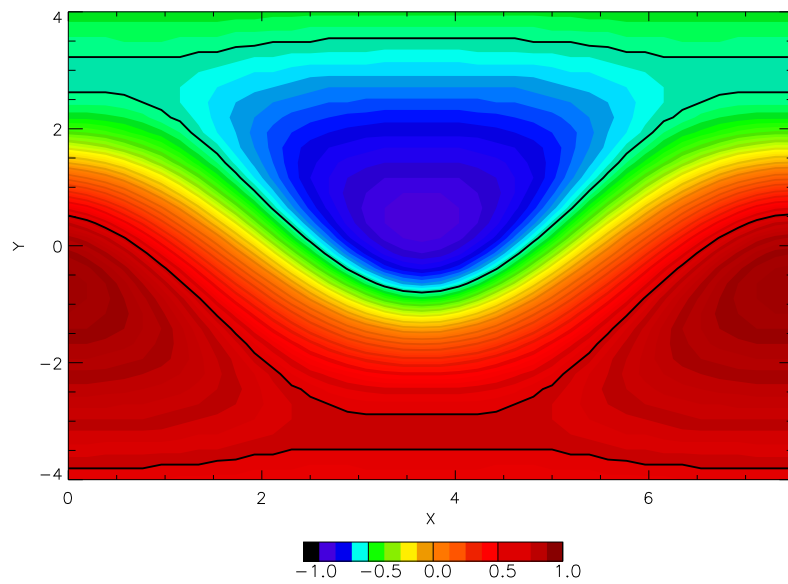


Figure 1: Map of the stream function of the meandering jet model. The isolines drawn in black represent the borderlines of the current. The jet core becomes a permeable barrier to cross-stream motion depending on the parameter values  $(\omega, \epsilon)$  of the time periodic perturbation.



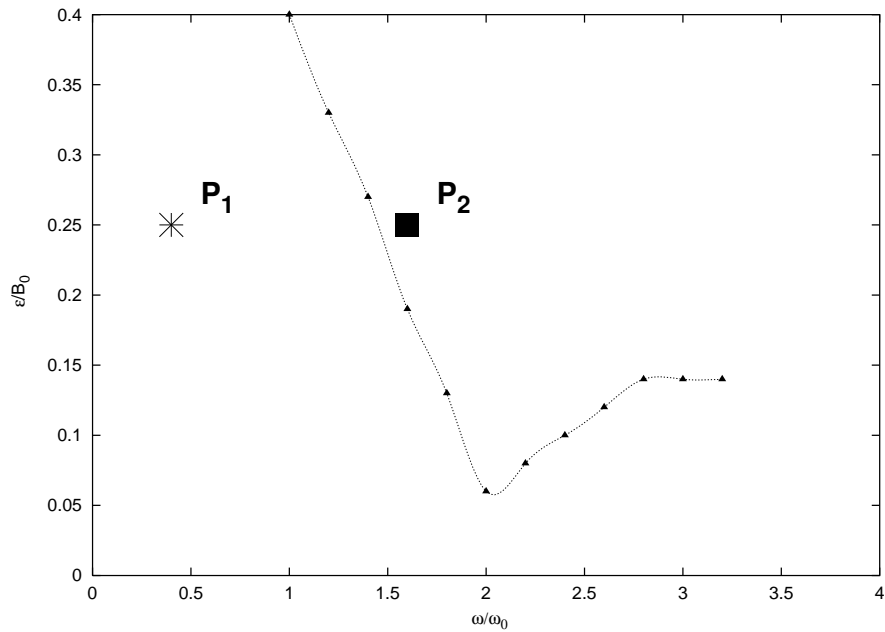
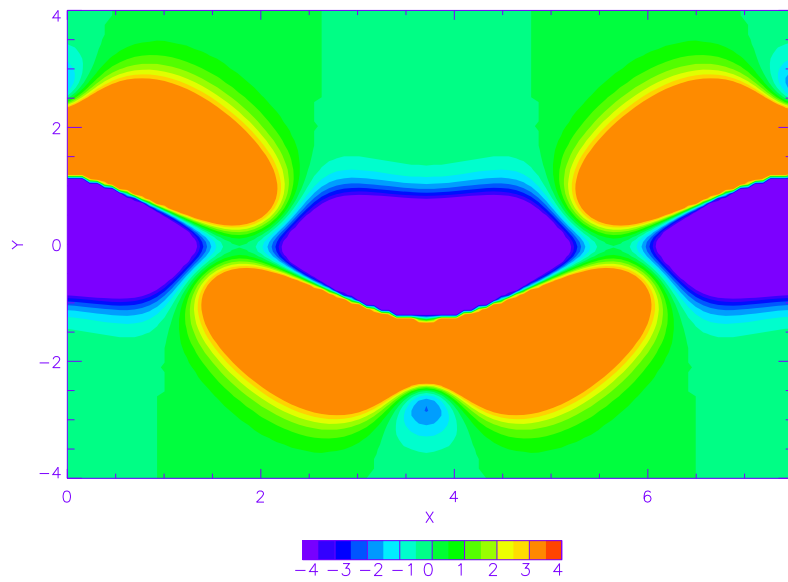


Figure 2: Critical curve in the parameter space  $(\omega, \epsilon)$  separating between “Melnikov regime” (below the curve), in which chaos is confined close to the separatrices, and “Chirikov regime” (above the curve), in which large-scale chaotic mixing occurs.  $P_1, (\omega, \epsilon) = (0.1, 0.3)$ , and  $P_2, (\omega, \epsilon) = (0.4, 0.3)$ , are the two points in the parameter space discussed in the Lagrangian simulations.  $\omega$  and  $\epsilon$  are adimensionalized with respect to  $\omega_0 = 0.25$  (pulsation of recirculating orbits next to the separatrices) and  $B_0 = 1.2$  (mean meander amplitude).

a)



b)

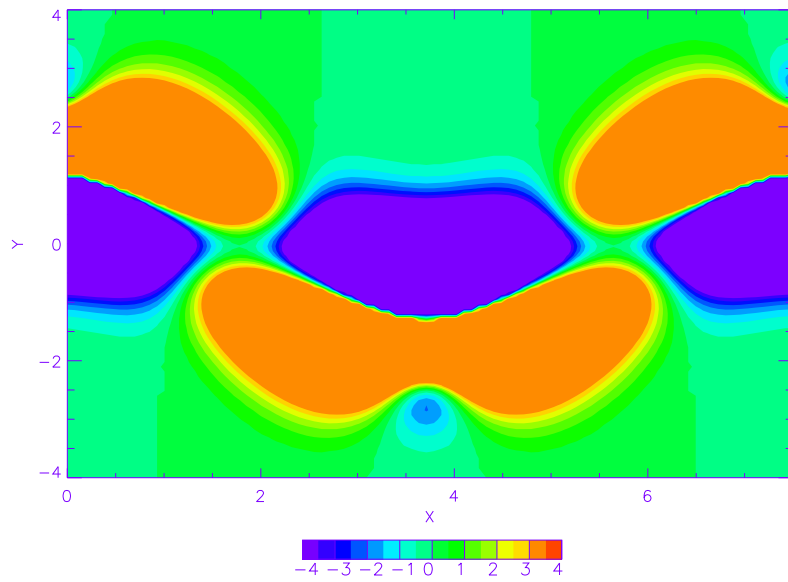


Figure 3: Okubo-Weiss parameter  $\lambda_0$  for the meandering jet system at the two parameter points  $P_1$  (a) and  $P_2$  (b) of Figure 2.

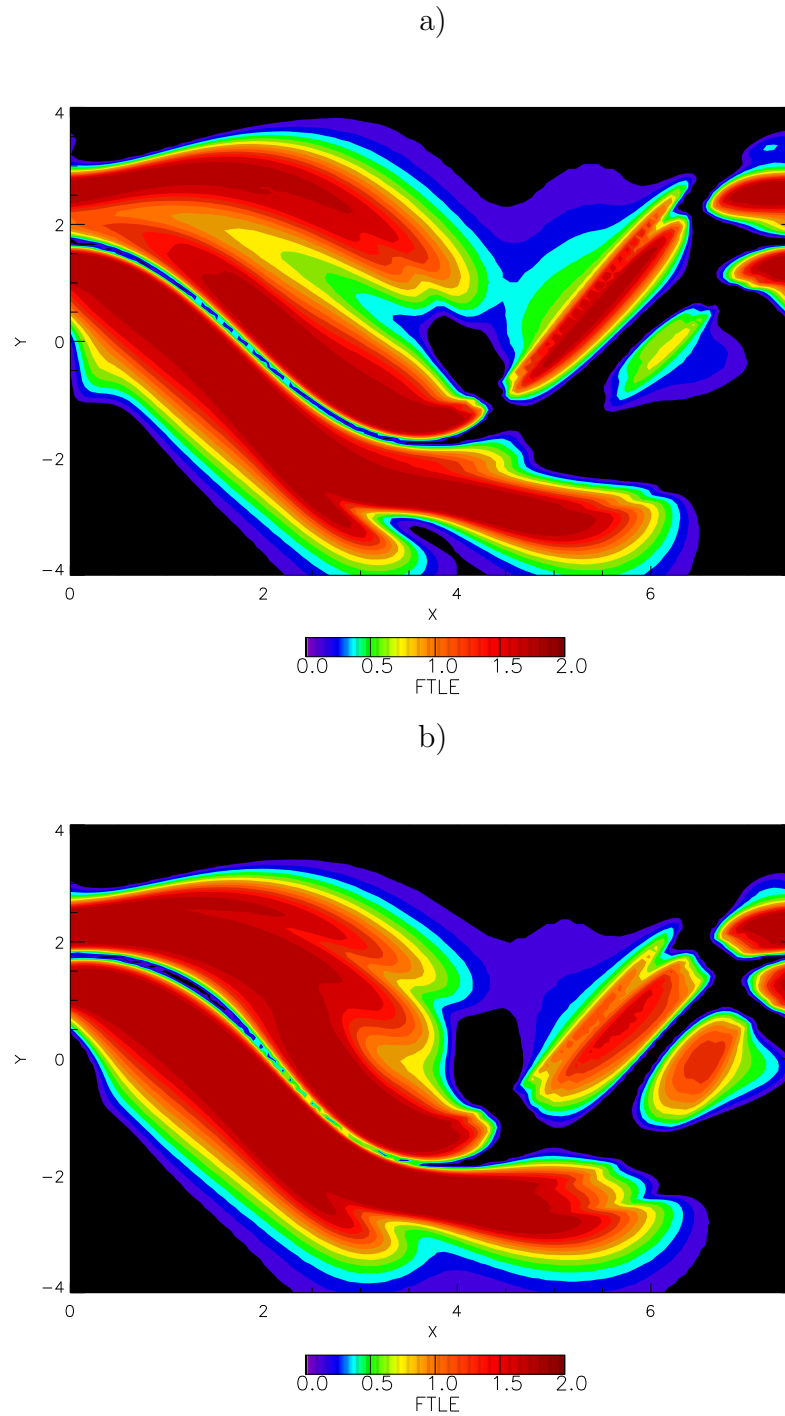


Figure 4: Finite time Lyapunov exponent  $\gamma_\tau(\mathbf{x})$  for the meandering jet system at the two parameter points  $P_1$  (a) and  $P_2$  (b). The number of particle pairs is 10000 with initial separation  $\delta/L = 1.9 \times 10^{-3}$  uniformly distributed on the periodic domain with spatial length  $L = 2\pi/k$  (with  $k = 0.84$ ). The time delay is  $\tau = \pi/\omega_0$ .

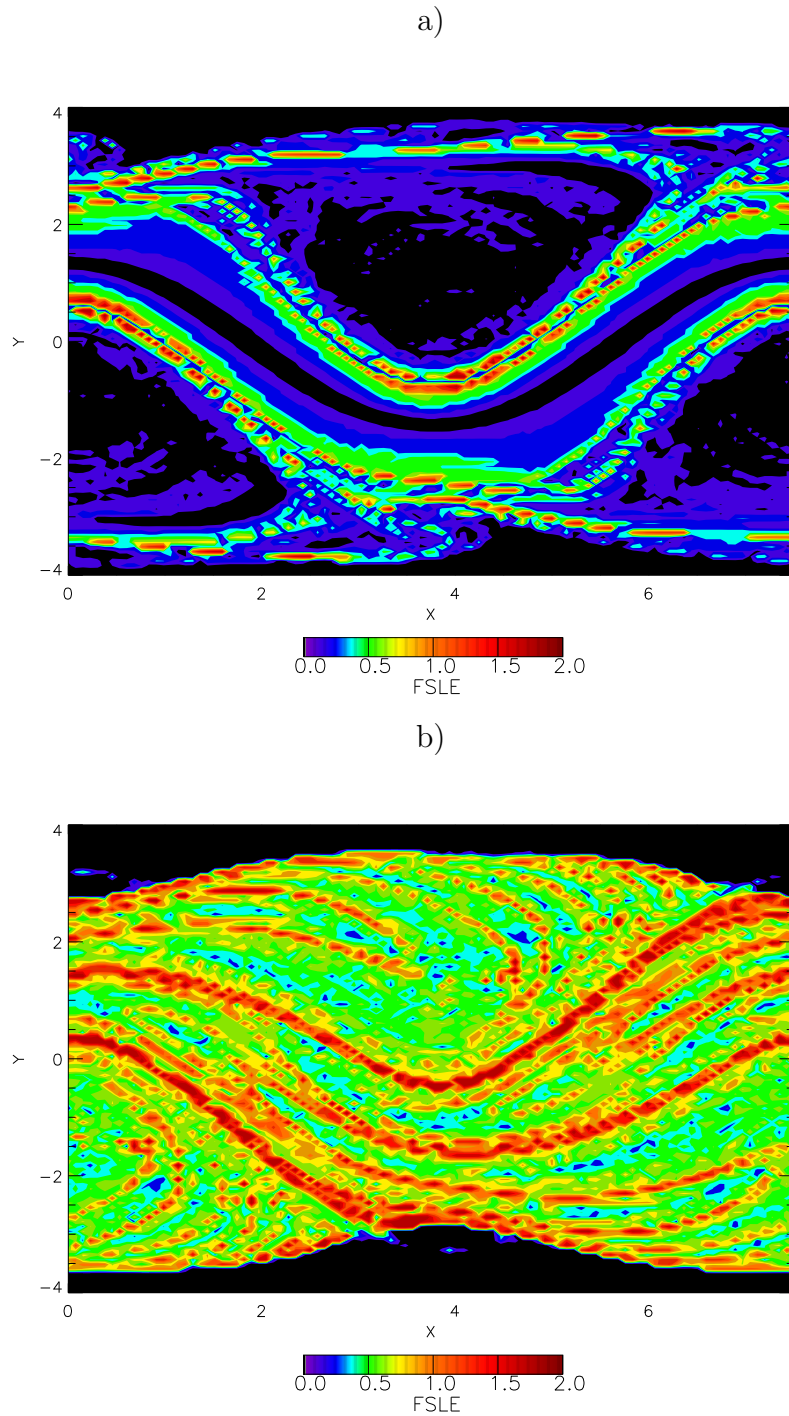


Figure 5: The local FSLE  $\lambda_r(\mathbf{x})$  for the meandering jet system at the parameter space points  $P_1$  (a) and  $P_2$  (b). The Lagrangian trajectories are the same of Figure 4. The amplification factor is  $r = 100$ . Only the particle pairs that reach a relative separation of  $r \cdot \delta \simeq 10^{-1}L$  give a positive signal in terms of  $\lambda(r)$ .

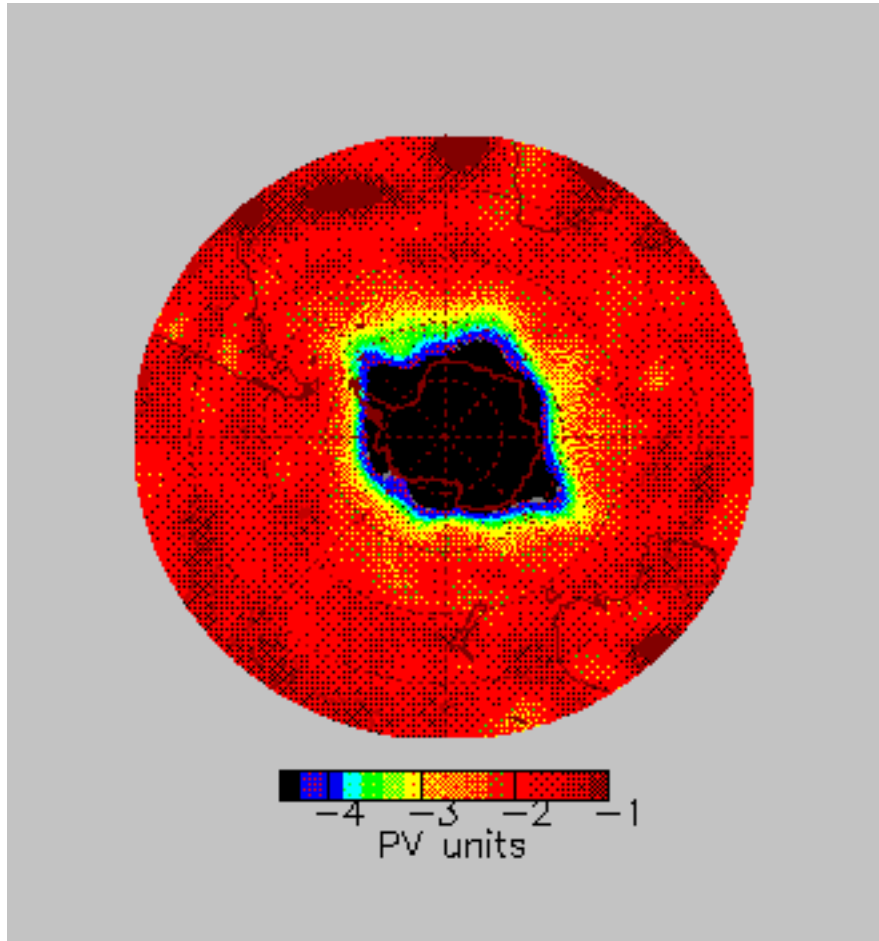


Figure 6: Map of potential vorticity (PV) taken at day June 30th 1997, relative to the 475K layer, southern hemisphere.

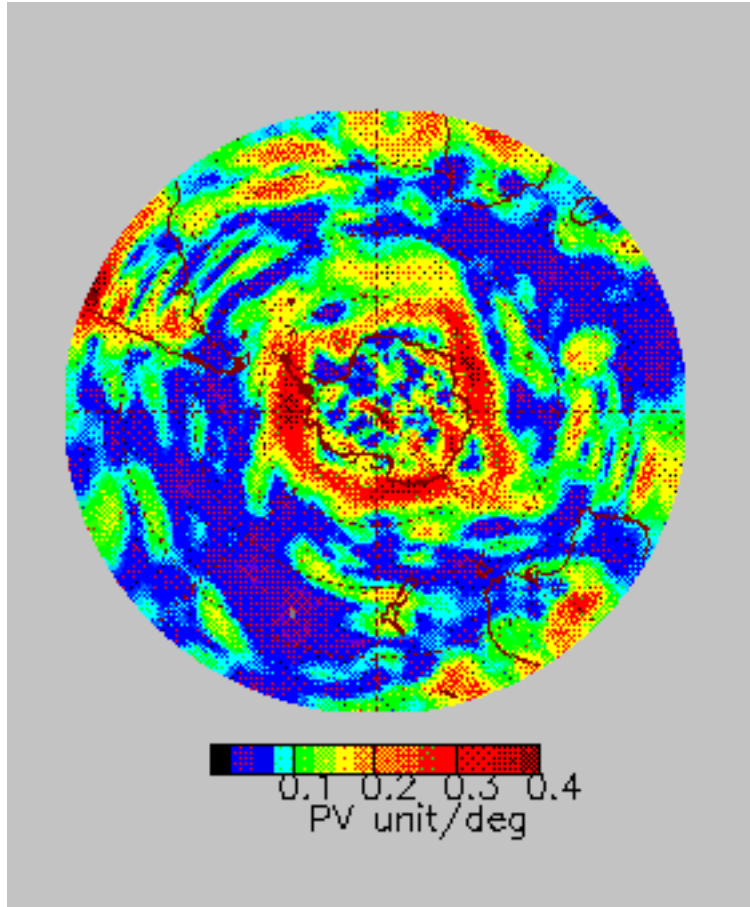


Figure 7: Map of the magnitude of the gradient of potential vorticity shown in Figure 6.

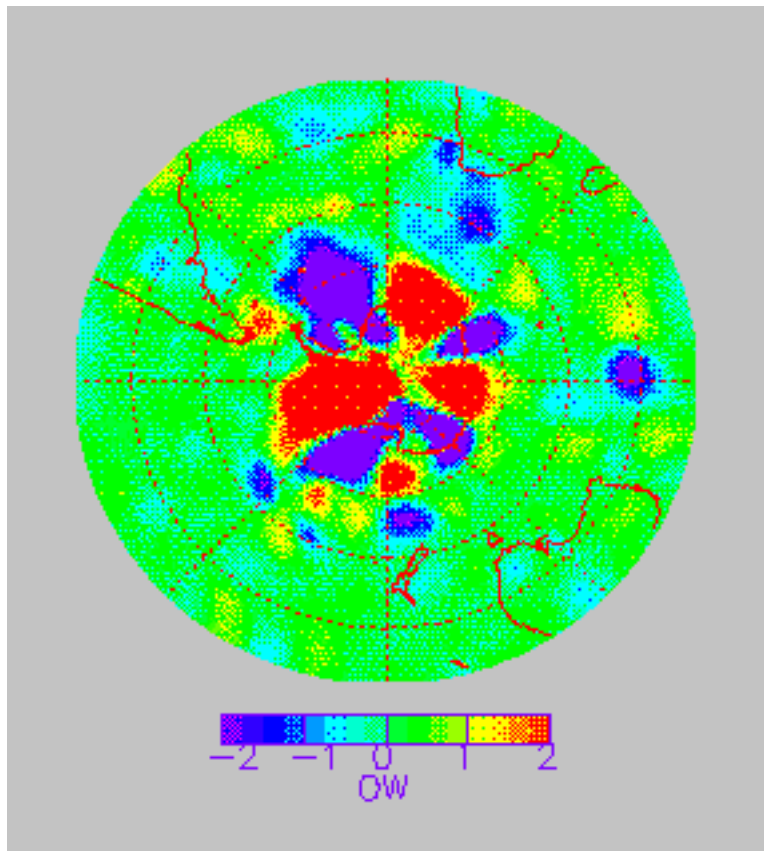


Figure 8: Okubo-Weiss indicator  $\lambda_0(\mathbf{x})$  for the analyzed wind fields corresponding to Figure 6, computed at the seventh day of the Lagrangian simulation, July 6th 1997.

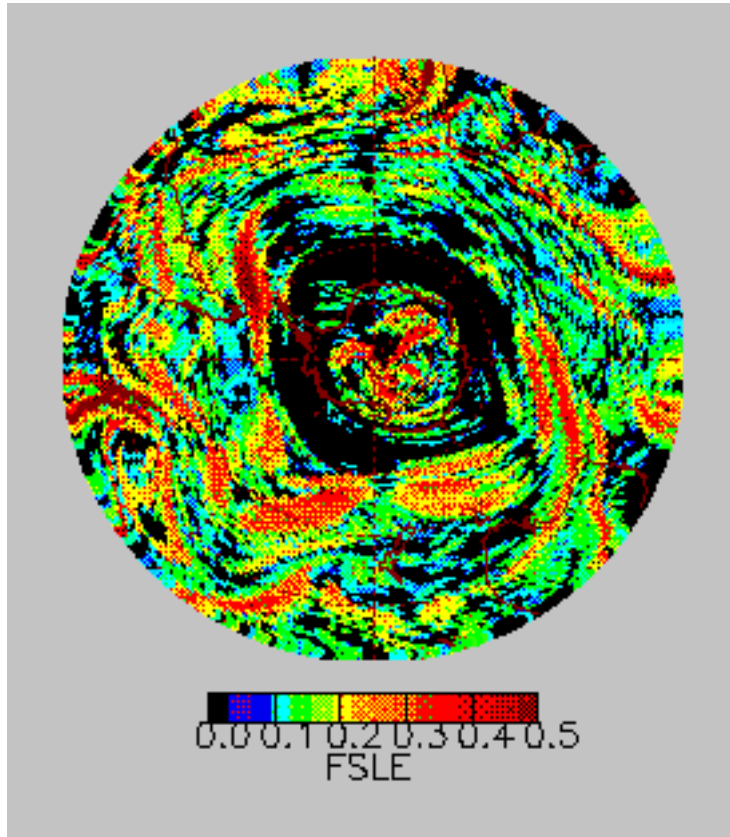


Figure 9: The local FSLE  $\lambda_r(\mathbf{x})$  map for the isentropic trajectory data set relative to the 475K layer. The initial distance between Lagrangian tracers is  $\delta \simeq 10$  km and the amplification factor is  $r = 10$ .